ADVANCED MATERIALS
www.advmat.de

Proteinticle/Gold Core/Shell Nanoparticles for Targeted Cancer Therapy without Nanotoxicity

Koo Chul Kwon, Ju Hee Ryu, Jong-Hwan Lee, Eun Jung Lee, Ick Chan Kwon, Kwangmeyung Kim, and Jeewon Lee**

For targeted and nanotoxicity-free cancer therapy, here we developed proteinticle/gold core/shell nanoparticles (PGCS-NP) through the surface engineering of proteinticle. Unlike synthetic nanoparticles, proteinticles are biological nanoparticles, i.e., nano-scale protein particles (e.g., viral capsid) that are self-assembled inside cells with constant structure and surface topology[1] and can be engineered to present specified peptides or proteins on their surface through genetic modification of the N- or C-terminus or internal region of the protein constituent.[1–3] Both poly-tyrosine with high reduction potential and affibody peptides with specific affinity for human epidermal growth factor receptor I (EGFR) were presented on the surface of hepatitis B virus capsid, and the subsequent Au^{+} reduction formed PGCS-NP (40 nm) that is dotted with many small gold NPs (1–3 nm). PGCS-NP shows excellent photothermal activity and high affinity for EGFR-expressing tumor cells. When intravenously injected into tumor-bearing mice, PGCS-NP effectively reached the EGFR-expressing tumor cells and caused severe tumor cell necrosis and significant reduction in tumor size upon NIR laser irradiation. Unlike gold NPs causing in vivo toxicity problems, PGCS-NP never caused any gross and histological lesions in major organs of mice, indicating that it is a safe and potent agent for photothermal therapy of cancer.

Despite the extensive research effort to develop synthetic nanoparticles for biomedical applications including cancer therapy, only a few synthetic nanoparticles (e.g., Abraxane, Doxil) have been clinically approved for therapeutics.[4,5] One of the reasons that make clinical translation of synthetic nanoparticles quite difficult is increasing concern about the nanoparticle-associated toxicity (nanotoxicity). Even developers and regulators remain uncertain about the nanotoxicity-associated risks in the environmental, health, and safety aspects.[6] A representative example is gold nanoparticle (NP) that is at the forefront of synthetic nanoparticles for therapeutic applications. Although bulk gold is generally considered biocompatible and inert,[7] recent studies have shown that gold NPs caused severe toxicity due to high-level accumulation in major organs like liver and spleen[7,8] and raised serious safety problems. In this study, we developed a novel strategy of cancer therapy using PGCS-NP to make gold NPs effectively metabolized and excreted after their therapeutic task is performed.

Photothermal therapy (PTT) of cancer that is based on the use of special materials (PTT agents) converting light to heat energy has the significant advantages over traditional surgical treatment or chemotherapy, because a non-invasive and localized treatment of cancer is possible.[9] Light irradiation to PTT agent localized in cancer causes hyperthermia of cancer cells at elevated temperature (41–47 °C) and finally results in necrosis of cancer cells that have low heat tolerance compared to normal cells.[10–12] Although a variety of PTT agents such as carbon-nanotubes,[13] quantum dots,[14] graphene oxide,[15] metal nanoparticles,[16] etc. have been studied, gold nanoparticles (NPs) are most widely used owing to its unique property of surface plasmon resonance (SPR) that results from coherent oscillations of conduction band electrons upon the absorption of visible light.[11]

An important issue of PTT is effective light penetration through tissues, and the laser with NIR wavelength favors effective tissue penetration.[11] Since the increase of gold NP size brings about red-shift of the light wavelength at which light absorption of gold NPs is maximized,[11] larger gold NPs are likely to be preferred in view of therapeutic efficacy of PTT. In other previous studies to enhance photothermal activity of gold NPs at NIR wavelenghth, the surface of large gold NPs was chemically modified,[17] or rod-shaped gold NPs were synthesized.[18] Reportedly, however, the larger size of gold NPs causes more severe in vivo toxicity due to the non-specific and long-term accumulation of NPs in tissues/organs: the gold NPs with a diameter more than 8 nm cannot pass through glomerular filtration;[16] a noticeable accumulation of gold NPs in reticulo-enthothelial system (RES) is observed when nanoparticle diameter exceeds 10 nm;[19] and the gold NPs with 40 to 80-nm diameter causes severe tissue damages in liver, spleen, and kidney after 28 days post intravenous injection.[20,21] Small nanopaticles are more easily cleared through renal excretion, but the gold NPs smaller than 2 nm cannot be used for PTT due to insufficient SPR effect.[22,23] There seems to be a narrow limitation in the size of gold NPs usable for effective PTT. Recently, Dreaden et al.[24] reported that the antibody-functionalized gold NPs with diameter of 40–50 nm have the maximum interaction with receptors [human epidermal growth factor receptor 2 (HER2)] of cancer cell.

Another major issue of PTT is targeted delivery of gold NPs to cancer cells. Enhanced targeting efficiency makes it

K. C. Kwon,[+] J.-H. Lee, E. J. Lee, Prof. J. Lee
Department of Chemical and Biological Engineering
College of Engineering
Korea University
Anam-Ro 145, Seoul 136–713, Republic of Korea
E-mail: leejw@korea.ac.kr
J. H. Ryu,[+] I. C. Kwon, Dr. K. Kim
Center for Theragnosis
Biomedical Research Institute
Korea Institute of Science and Technology
39–1 Hawolgok-dong, Seongbuk-gu, Seoul 136–791, Republic of Korea
E-mail: kim@kist.re.kr
[+]These authors contributed equally to this work.

DOI: 10.1002/adma.201401499

possible to reduce the amount of gold NPs without decreasing the therapeutic effect of PTT, contributes to the decrease in in vivo toxicity, and hence makes PTT more useful in cancer therapy. Often the gold NP surface has been chemically modified to attach specified biomolecules (peptides or antibodies with binding affinity for cancer cells).[19] However, due to the chemical attachment in a random fashion, surface density, orientation, conformation, and activity of the biomolecules are not controllable on the NP surface, which still remains an unsolved obstacle to increasing cancer targeting efficiency. It is noticeable that Lee et al.,[1] Park et al.[2] and Lee et al.[3] recently reported an efficient engineering method to present active peptides and antibodies on the surface of proteinticles that were used for in vitro bioassays. Furthermore, hydrophobic adsorption of serum proteins can either increase hydrodynamic diameter of gold NPs or change the activity of gold NP-bound peptides/antibodies and therefore affect the interaction with cancer cells.[20] Consequently, the critical factors that should be improved to solve the traditional problems of PTT using gold NPs are summarized as: 1) photothermal activity of gold NPs at NIR wavelength that is effective for tissue penetration, 2) targeted delivery of gold NPs to cancer cells, and 3) in vivo safety of gold NPs without accumulation problems in organs such as liver, spleen, and kidneys.

When expressed in *Escherichia coli*, the hepatitis B virus (HBV) core protein (subunit of capsid) truncated after 149th residue assembles into a core shell capsid that contains 240 subunits and has an overall diameter of 36 nm.[25,26] The dimer clustering of subunits produces 120 immunogenic spikes on the surface of each capsid, and the outermost spike tip corresponds to the loop segment consisting of the residues from D78 to D83 of the core protein (**Figure 1**A). Figure 1A schematically shows the surface engineering of HBV-capsid based proteinticle: we inserted the tandem repeated affibody peptides with specific affinity for EGFR into the surface loop segment by replacing P79A80 and also added hexahistidine (H_6), biotinylated peptide (BP), and hexatyrosine (Y_6) to the N-terminus of the core protein. The modified HBV core proteins are expressed and self-assembled in *E. coli* to form the engineered proteinticle, on the surface of which both of the EGFR-affibodies and H_6-BP-Y_6 peptides are displayed according to the surface topology of HBV capsid.[2] The engineered proteinticles were mixed with Tris buffer containing chloro(trimethyl-phosphine)gold(I), and subsequently gold ions (Au^+) are reduced to gold by the high reduction potential of Y_6 residues, consequently leading to the formation of affibody-PGCS-NP. Each PGCS-NP is dotted with many small gold NPs (1–3 nm in diameter), which was confirmed by transmission electron microscope images (Figure 1B) and energy dispersive X-ray (EDX) spectroscopy analysis (Supporting Information (SI) Figure S1A). Dynamic light scattering (DLS) analysis shows the uniform size distribution (about 40 nm in diameter) of PGCS-NP (SIFigure S1B). Furthermore, it is noticeable that bare gold NPs (40 nm) are heavily aggregated either upon the concentration in distilled water or upon the buffer exchange to PBS (SI Figure S2A), while PGCS-NPs do not undergo any aggregation even when concentrated in PBS buffer (SI Figure S2B). This is presumably because the surface charge of proteinticle and/or the small surface area of gold reduce hydrophobic inter-particle aggregation.

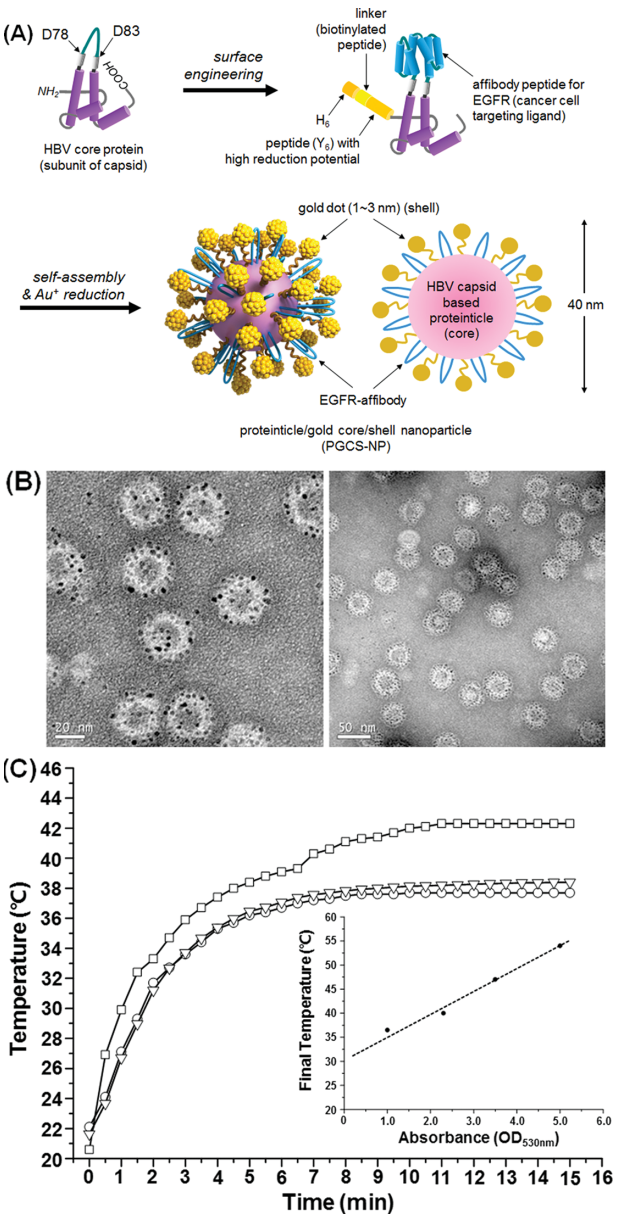

Figure 1. Proteinticle engineering for PGCS-NP synthesis and photothermal activity of PGCS-NP. (A) A schematic showing genetically modified subunit protein of HBV capsid and biosynthesis of PGCS-NP by Au^+ reduction. (B) TEM images of synthesized and purified PGCS-NP. (C) Photothermal activity of PGCS-NP (□) and gold NPs with diameter of 5- (∇) and 40 nm (○) upon NIR (530 nm) irradiation.

The absorbance of PGCS-NP and 40-nm gold NP is maximized at a nearly identical wavelength of 530 nm (SI Figure S1C), indicating that the light absorption property of PGCS-NP is determined by the whole size of PGCS-NP (about 40 nm), not by the size of individual gold dots. Upon NIR laser (655 nm) irradiation, the temperature of PGCS-NP solution increases to around 42 °C within 10 min, while the final temperature of the solution containing only gold NP (5 or 40 nm) is lower than 39°C although the gold concentration is identical in the solutions of PGCS-NP and gold NP (Figure 1C). The temperature increment by the photothermal activity of PGCS-NP

Adv. Mater. **2014**,
DOI: 10.1002/adma.201401499

is linearly proportional to the gold concentration of PGCS-NP, and the final temperature of PGCS-NP solution is higher than 52 °C at the highest gold (or PGCS-NP) concentration tested (inset plot of Figure 1C). [The concentration of gold NP was estimated by measuring the absorbance at 520 nm using the reference data (SI Figure S7), presuming that the magnitude of absorbance measured at the same 520 nm is proportional to the concentration of gold NPs.[27] The enhanced photothermal activity of PGCS-NP seems to result from collective plasmon resonance of small gold dots on PGCS-NP.[28] Reportedly, collective plasmon resonance of many adjacent small NPs increases total heat generation and also creates hot spots where heating intensity is greatly enhanced.[29]

Affibody-presenting PGCS-NP (named affibody-PGCS-NP) specifically bound to EGFR-expressing cancer cells (MDA-MB-468 cells).[30] When incubated with in vitro MDA-MB-468 cells, fluorescence-labeled affibody-PGCS-NP showed strong cellular fluorescence signals (**Figure 2**A-b), whereas the cellular fluorescence is almost negligible with affibody-free PGCS-NP (Figure 2A-a). In addition, MDA-MB-468 cells that are pretreated using Cetuximab (anti-EGFR monoclonal antibody) to block the binding of affibody-PGCS-NP to EGFR show remarkably reduced cellular fluorescence (Figure 2A-c). In computed tomography (CT) examinations, evident accumulation and retention of affibody-PGCS-NP in the tumor was visualized at 2 h after the intratumoral injection into MDA-MB-468 tumor in

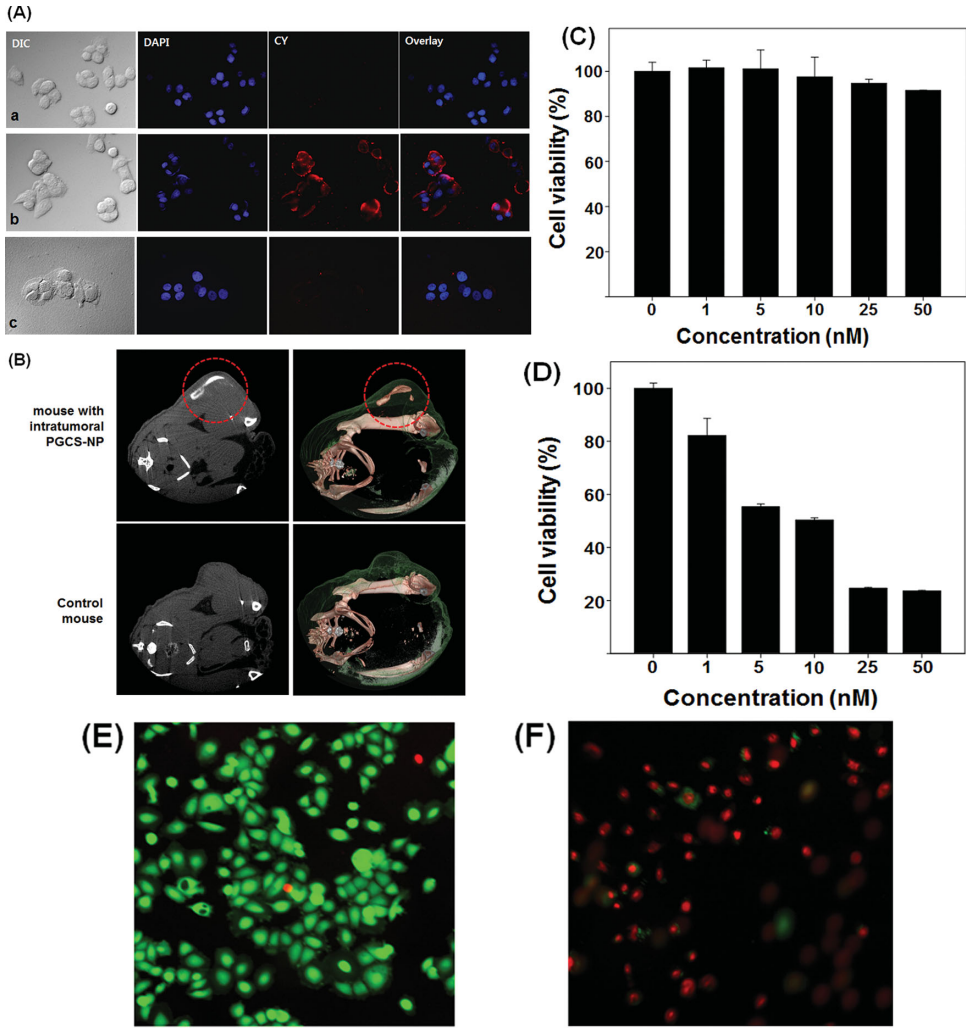

Figure 2. Specific affinity of PGCS-NP for EGFR-expressing cancer (MDA-MB-468) cells in vitro or in mice and in vitro performance of photothermal ablation. Cellular images after incubated with (A-a) affibody-free PGCS-NP without Cetuximab pretreatment, (A-b) affibody-PGCS-NP without Cetuximab pretreatment, and (A-c) affibody-PGCS-NP with Cetuximab pretreatment in MDA-MB-468 cells. After labeled by Cy5.5, affibody-free PGCS-NP or affibody-PGCS-NP (2.5 μg/mL) was incubated with MDA-MB-468 cells for 10 min. Cetuximab (4.0 μM) was treated to the culture medium at 72 h before affibody-PGCS-NP treatment. Nuclei were counterstained with DAPI (blue). (B) Cross-sectional microcomputed tomography images and its reconstructed three dimentional images at 2 h after the intratumoral injection of affibody-PGCS-NP or PBS (control) into MDA-MB-468 tumor in mice. The contrast of tumor image (in dotted circle) is enhanced due to affibody-PGCS-NP deposition. Cell viability determined by CCK-8 assay: (C) MDA-MB-468 cells were incubated with different concentrations of affibody-PGCS-NP without laser irradiation. (D) MDA-MB-468 cells were incubated with different concentrations of affibody-PGCS-NP under the 655-nm laser irradiation for 20 min (24 W/cm^2). Fluorescence images of the cells incubated under the laser irradiation (E) with or (F) without affibody-PGCS-NP (25 nM) stained by Calcein AM/PI.

mice (Figure 2B). The results of Figure 2A and 2B suggest high binding affinity of affibody-PGCS-NP for the EGFR-expressing tumor cells.

MDA-MB-468 cells that were incubated with affibody-PGCS-NP for 6 h without NIR irradiation remained more than 90% viable at the concentrations of affibody-PGCS-NP up to 50 nM, as measured by a Cell Counting Kit-8 (CCK-8) assay (Figure 2C). However, when the cells were treated with affibody-PGCS-NP for 1 h and then exposed to NIR irradiation (655 nm, 24 W/cm^2, 20 min), cell death significantly increased as the concentration of affibody-PGCS-NP increased (Figure 2D). Fluorescence images of Calcein AM and propidium iodide (PI)[31] also confirmed severe necrosis of the tumor cells caused by affibody-PGCS-NP plus irradiation, although almost all the cancer cells exposed to NIR laser alone were viable (Figure 2E and 2F). After bound to affibody-PGCS-NP, in vitro cancer cells were effectively killed under NIR laser irradiation (Figure 2C to 2F), indicating a potency of affibody-PGCS-NP as an in vivo photoabsorber for targeted and photothermal therapy of cancer.

Intravenous injection of fluorescence-labeled affibody-PGCS-NP into MDA-MB-468 tumor-bearing mice resulted in higher NIR fluorescence intensity in the tumor compared to the injection of affibody-free PGCS-NP. When the tumor size reached approximately 5 mm in diameter, the mice were intravenously administered with affibody-PGCS-NP or affibody-free PGCS-NP and imaged at multiple time points for 24 h (**Figure 3**A, SI Figure S3). The NIR fluorescence signals gradually increased and reached the highest level at 12 h after the intravenous injection. In particular, the NIR fluorescence intensity of affibody-PGCS-NP in the tumor was apparently higher than that of affibody-free PGCS-NP at all time points (Figure 3B), indicating that the EGFR-specific affibody-PGCS-NP is significantly effective for cancer targeting in vivo.

The efficacy of affibody-PGCS-NP in photothermal therapy of cancer was estimated with NIR laser irradiation. MDA-MB-468 tumors in the mice that were intravenously injected with affibody-PGCS-NP were dramatically ablated after NIR laser irradiation, whereas laser exposure alone caused negligible damage on the tumor (Figure 3C, SI Figure S4). Tumoricidal effect of the photothermal treatment using intravenously injected affibody-PGCS-NP was histologically assessed (Figure 3D). In hematoxylin and eosin (H&E) stains, the tumors treated with affibody-PGCS-NP plus irradiation exhibited a wide range of cell death in the entire region, while most tumor cells were intact in the tumor treated with affibody-PGCS-NP alone. From Figure 3A to 3D, it is quite clear that affibody-PGCS-NP is highly effective in targeted and photothermal therapy of cancer.

The histological effect of affibody-PGCS-NP (0.46 mg gold/100-μL distilled water) and 20-nm gold NP (0.46 mg/100-μL distilled water) on five major organs (liver, lung, spleen, kidney, and heart) of healthy mice was monitored at 24 h after intravenous injection. Noticeable tissue damage was detected in liver and kidney of the mice injected with gold NP: diffuse ballooning degeneration of hepatocytes and focal tubular necrosis

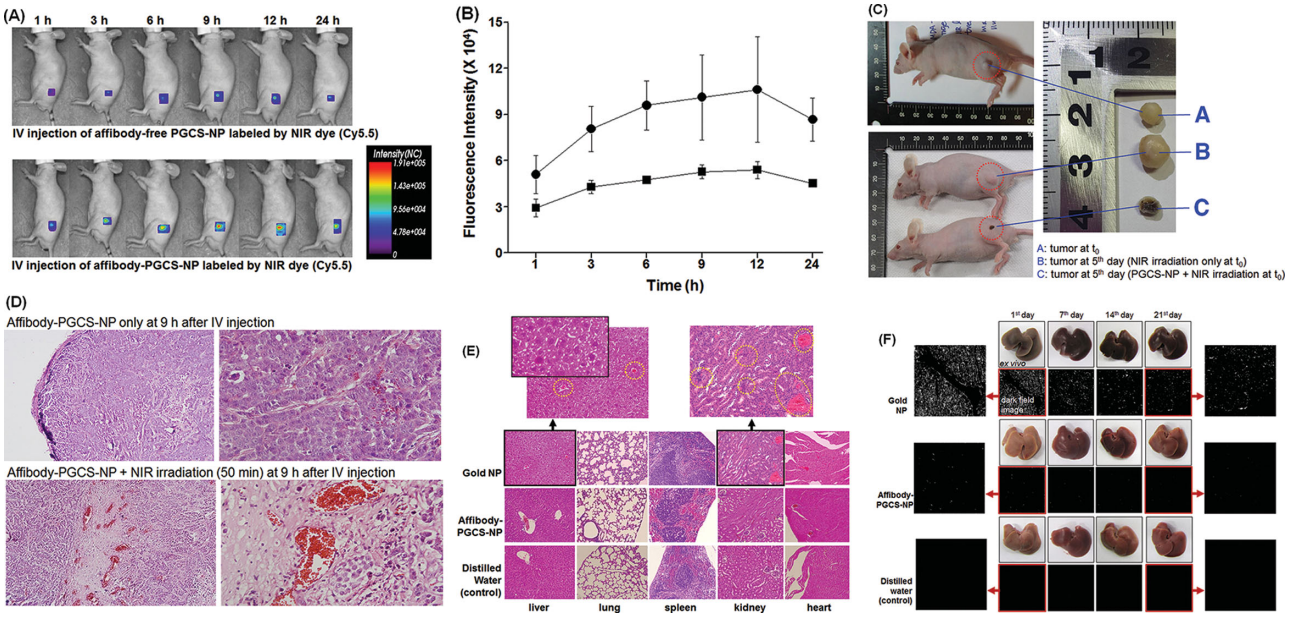

Figure 3. In vivo tumor targeting, photothermal cancer therapy, and biocompatibility of PGCS-NP after intravenous injection to MDA-MB-468 tumor-bearing mice. (A) In vivo NIR fluorescence images of subcutaneous MDA-MB-468 tumor-bearing mice (n = 4) at predetermined time points after intravenous injection of affibody-free PGCS-NP or affibody-PGCS-NP, both of which are Cy5.5-labeled. Higher NIR fluorescence intensity was visualized in MDA-MB-468 tumors when intravenously injected with affibody-PGCS-NP compared to affibody-free PGCS-NP. (B) Time-course NIR fluorescence intensity in the tumor region of MDA-MB-468 tumor-bearing mice treated with affibody-PGCS-NP (circle) or affibody-free PGCS-NP (square). (C) Representative pictures of MDA-MB-468 tumor-bearing mice and excised tumors after in vivo photothermal therapy. (D) H&E staining images of MDA-MB-468 tumors treated with or without the 655-nm laser irradiation at 9 h after intravenous injection of affibody-PGCS-NP. (E) H&E staining images of liver, lung, spleen, kidney, and heart at 1 day after affibody-PGCS-NP (4.6 mg gold/mL), 20-nm gold NP (4.6 mg/mL), or distilled water was intravenously injected into healthy mice. Distinct tissue damage was histologically detected in liver and kidney of mice injected with 20-nm gold NP. (F) Macroscopic appearance and dark field images of the excised livers at 1 day, 7 days, 14 days, and 21 days after the intravenous injection of affibody-PGCS-NP (9.2 mg gold/mL), 20-nm gold NP (9.2 mg/mL), or distilled water was intravenously injected into healthy mice.

Adv. Mater. **2014**,
DOI: 10.1002/adma.201401499

in kidney, whereas no histopathological abnormalities were found in five major organs of the mice injected with affibody-PGCS-NP as compared to control (Figure 3E). The biodistributions of gold in liver, kidney, and spleen of healthy mice were examined again for a longer period (3 weeks) after intravenous injection of affibody-PGCS-NP (0.92 mg gold/100-μL distilled water) and 20-nm gold NP (0.92 mg/100-μL distilled water). Macroscopic ex vivo images of the organs were obtained at 1 day, 7 days, 14 days, and 21 days post injection (Figure 3F, SI Figure S5). When affibody-PGCS-NP was intravenously injected, no visible change was observed in the excised livers, compared to the livers injected with distilled water (control). In the case of 20-nm gold NP, however, a dark brownish discoloration of the excised livers was observed at all the time points for 3 weeks, indicating the extensive liver damage. The reason for the severe liver damage by 20-nm gold NP is partly explained by the results of dark field microscopy, showing a high-level and prolonged accumulation of 20-nm gold NPs in the liver, which is presumably due to the large size of gold NP as already reported on hepatotoxicity of gold NPs.[16,32–34]

PGCS-NP is a nanocluster consisting of 240 protein subunits and many small gold dots. Each protein subunit of PGCS-NP could be spontaneously denatured in liver, leading to disassembly of PGCS-NP. From the results of Figure 3F, it is understood that PGCS-NP is initially accumulated in the liver, but as PGCS-NP is disassembled with time, the small gold dots released from the disassembled PGCS-NP excreted from the liver. This is also explained by the similar finding (SI Figure S5) that the accumulation of gold was detected in the kidney analyzed at 1 day after the injection of affibody-PGCS-NP but not detectable in the kidney at other time points, suggesting that the released small gold dots were easily cleared through renal excretion after 1 day post injection,[21] as also evidenced in this study (SI Figure S6).

Unlike surgical treatment or chemotherapy, PTT is a non-invasive and localized treatment of cancer. Gold NPs with unique SPR property are currently the most popular PTT agent, but the following important issues remain to be solved to make the gold-NP based PTT widely used in the medical field of cancer therapy: 1) photothermal activity of gold NPs at NIR wavelength that is effective for tissue penetration, 2) targeted delivery of gold NPs to cancer cells, and 3) in vivo toxicity of gold NPs by prolonged accumulation in organs such as liver, spleen, and kidneys. As a solution to the critical issues above, here we proposed the use of PGCS-NP with strong and specific affinity for EGFR on cancer cells, at the surface of which small (1 to 3-nm) gold NPs are densely dotted. Although used as a cancer targeting ligand for proof-of-concept in this case, the EGFR-affibody on the surface of PGCS-NP can be easily switched to another peptide in accordance with specific target molecules on cancer cells. Due probably to collective plasmon resonance among the small gold NPs, PGCS-NP showed excellent photothermal activity, compared to gold NPs. When intravenously injected into tumor-bearing mice, affibody-presenting PGCS-NP was effectively delivered to EGFR-expressing tumor cells, and the localized irradiation of NIR laser caused both severe tumor cell necrosis and remarkable tumor size reduction. We also confirmed that gold NPs caused extensive and histological damages to liver and kidney of healthy mice, while in the case of PGCS-NP no visible macroscopic and histological change was observed in major organs (liver, spleen, and kidney) of healthy mice for 3 weeks after intravenous injection. It seems that in vivo spontaneous denaturation of protein subunits makes PGCS-NP disassembled into many tiny gold dots that can be rapidly excreted from liver and kidney due to their small size, indicating that PGCS-NP can be used as a safe PTT agent for targeted cancer therapy without in vivo toxicity problems.

Supporting Information

Supporting Information, including experimental protocols, is available from the Wiley Online Library or from the author.

Acknowledgements

This study was supported by the 2012 NLRL (National Leading Research Lab.) Project (grant no. 2012R1A2A1A01008085) (the main project that supported this work), the Basic Science Research Program (ERC program, grant no. 2010-0029409) of the National Research Foundation of Korea (NRF), and KIST Intramural project (Theragnosis).

Received: April 3, 2014
Revised: May 8, 2014
Published online:

[1] J.-H. Lee, H. S. Seo, J. A. Song, K. C. Kwon, E. J. Lee, H. J. Kim, E. B. Lee, Y. J. Cha, J. Lee, *ACS Nano* **2013**, *7*, 10879–10886.
[2] J. S. Park, M. K. Cho, E. J. Lee, K.-Y. Ahn, K. E. Lee, J. H. Jung, Y. Cho, S-S. Han, Y. K. Kim, J. Lee, *Nat. Nanotechnol.* **2009**, *4*, 259–264.
[3] E. J. Lee, K. Y. Ahn, J.-H. Lee, J. S. Park, J. A. Song, S. J. Sim, E. B. Lee, Y. J. Cha, J. Lee, *Adv. Mater.* **2012**, *24*, 4739–4744.
[4] D. Peer, J. M. Karp, S. Hong, O. C. Farokhzad, R. Margalit, R. Langer, *Nat. Nanotechnol.* **2007**, *2*, 751–760.
[5] A. Z. Wang, R. Langer, O. C. Farokhzad, *Annu. Rev. Med.* **2012**, *63*, 185–198.
[6] National Research Council, *A Research Strategy for Environmental, Health, and Safety Aspects of Engineered Nanomaterials*, The National Academies Press, Washington, DC, USA **2012**.
[7] S. C. Yah, *Biomed. Res.* **2013**, *24*, 400–413.
[8] N. Khlebtsov, L. Dykman, *Chem. Soc. Rev.* **2011**, *40*, 1647–1671.
[9] G. Shan, R. Weissleder, S. A. Hilderbrand, *Theranostics* **2013**, *3*, 267–274.
[10] C. M. Philipp, E. Rohde, H. P. Berlien, *Semin. Surg. Oncol.* **1995**, *11*, 290–298.
[11] X. Huang, P. K. Jain, I. H. El Sayed, M. A. El Sayed, *Lasers Med. Sci.* **2008**, *23*, 217–228.
[12] B. Van de Broek, N. Devoogdt, A. D'Hollander, H. L. Gijs, K. Jans, L. Lagae, S. Muyldemans, G. Maes, G. Borghs, *ACS Nano* **2011**, *5*, 4319–4328.
[13] N. W. S. Kam, M. O'Connell, J. A. Wisdom, H. Dai, *Proc. Natl. Acad. Sci. U S A* **2005**, *102*, 11600–11605.
[14] M. Chu, X. Pan, D. Zhang, Q. Wu, J. Peng, W. Hai, *Biomaterials* **2012**, *33*, 7071–7083.
[15] O. Akhavan, E. Ghaderi, S. Aghayee, Y. Fereydooni, A. Talebi, *J. Mater. Chem.* **2012**, *22*, 13773–13781.
[16] X. D. Zhang, D. Wu, X. Shen, P. X. Liu, F. Y. Fan, S. J. Fan, *Biomaterials* **2012**, *33*, 4628–4638.
[17] J. Nam, N. Won, H. Jin, H. Chung, S. Kim, *J. Am. Chem. Soc.* **2009**, *131*, 13639–13645.

[18] F. Kim, J. H. Song, P. Yang, *J. Am. Chem. Soc.* **2002**, *124*, 14316–14317.
[19] M. Bartneck, T. Ritz, H. A. Keul, M. Wambach, J. Bomemann, U. Gbureck, J. Ehling, T. Lammers, F. Heymann, N. Gassler, T. Lüdde, C. Trautwein, J. Groll, F. Tacke, *ACS Nano* **2012**, *6*, 8767–8777.
[20] M. R. Papasani, G. Wang, R. A. Hill, *Nanomedicine* **2012**, *8*, 804–814.
[21] Z. Chen, L. Michael, Q. Yanping, S. Xiankai, Z. Jie, *Angew. Chem. Int. Ed.* **2011**, *123*, 3226–3230.
[22] J. Song, D. Kim, D. Lee, *Langmuir* **2011**, *27*, 13854–13860.
[23] T. A. El-Brolossy, T. Abdallah, M. B. Mohamed, S. Abdallah, K. Easawi, S. Negm, H. Talaat, *Eur. Phys. J. Spec.* **2008**, *153*, 361–364.
[24] E. C. Dreaden, A. M. Alkilany, X. Huang, C. J. Murphy, M. A. El-Sayed, *Chem. Soc. Rev.* **2012**, *41*, 2740–2779.
[25] K. Nord, E. Gunneriusson, J. Ringdahl, S. Ståhl, M. Uhlén, P. A. Nygren, *Nat. Biotechnol.* **1996**, *15*, 772–777.
[26] Z. Miao, G. Ren, H. Liu, L. Jiang, Z. Cheng, *Bioconjug. Chem.* **2010**, *21*, 947–954.
[27] C. Burda, X. Chen, R. Narayanan, M. A. El-Sayed, *Chem. Rev.* **2005**, *105*, 1025–1102.
[28] B. N. Khlebtsov, V. A. Khanadeyev, N. G. Khlebtsov, *Physical Optics* **2008**, *104*, 282–294.
[29] A. O. Govorov, W. Zhang, T. Skeini, H. Richardson, J. Lee, N. A. Kotov, *Nanoscale Res. Lett.* **2006**, *1*, 84–90.
[30] J. H. Ryu, M. Shin, S. A. Kim, S. Lee, H. Kim, H. Koo, B. S. Kim, H. K. Song, S. H. Kim, K. Choi, I. C. Kwon, H. Jeon, K. Kim, *Biomaterials* **2013**, *34*, 9149–9159.
[31] K. Hengte, W. Jinrui, D. Zhifei, J. Yushen, Q. Enze, X. Zhanwen, G. Caixin, Y. Xiuli, L. Jinbin, *Angew. Chem. Int. Ed.* **2011**, *50*, 3017–3021.
[32] M. Longmire, P. L. Choyke, H. Kobayashi, *Nanomedicine* **2008**, *3*, 703–717.
[33] W. S. Cho, M. Cho, J. Jeong, M. Choi, B. S. Han, H. S. Shin, J. Hong, B. H. Chung, J. Jeong, M. H. Cho, *Toxicol. Appl. Pharmacol.* **2010**, *245*, 116–123.
[34] Y. Pan, S. Neuss, A. Leifert, M. Fischler, F. Wen, U. Simon, G. Schmid, W. Brandau, W. Jahnen-Dechent, *Small* **2007**, *3*, 1941–1949.

Adv. Mater. **2014**,
DOI: 10.1002/adma.201401499